Measuring the Properties of the Gaussian Beam in the Advanced Laboratory - L7

Grzegorz Jędrzejowski

27 February 2025

The detailed analysis of the light beam's intensity profile led to the identification of the Gaussian beam parameters in all analyzed cases. However, due to limited datasets, some parameters could not be reliably determined. To obtain all the desired parameters with higher accuracy, new measurements should be conducted with an increased number of data points and a modified methodology to ensure higher density near the focal point.

1 Introduction

1.1 Gaussian Beam

A Gaussian beam is a type of electromagnetic wave with an intensity profile that follows a Gaussian distribution, meaning it has a single peak at its center that gradually tapers off towards the edges. Gaussian beams maintain their shape over relatively long distances and they exhibit minimal diffraction. They are widely applicable in fields like telecommunications, imaging, and materials processing. A Gaussian beam with optical power (P), waist function as a function of distance ($w(z)$), and distance from the beam center (r) follows the intensity profile of a Gaussian function [1]:

$$I(r,z) = \frac{2P}{\pi w(z)^2} \exp(-2\frac{r^2}{w(z)^2}). \quad (1)$$

1.2 Properties of the Gaussian Beam

The waist is an important property of a Gaussian beam and it follows the following relation:

$$w(z) = w_0\sqrt{1 + M^2(\frac{z-z_0}{z_R})^2}. \quad (2)$$

In Equation (2) the parameter w_0 represents the beam waist at its narrowest point, z is a variable representing the propagation distance, z_0 denotes the offset of w_0, and z_R is called Rayleigh length:

$$z_R = \frac{\pi w_0^2}{\lambda}, \quad (3)$$

where λ represents the wavelength of the light beam. The physical interpretation of this parameter is that it determines the length over which the beam can propagate without diverging significantly [1]. The M^2 parameter, also known as the beam quality factor, quantifies beam quality with a single value and predicts beam radius evolution. This is done by substituting the wavelength with M^2 times the wavelength in all relevant equations. Its value is 1 for perfect Gaussian beams and greater than 1 for other types of beams [2].

1.3 Obtaining beam parameters

The beam will be measured in terms of its intensity, as shown in Equation (1), using a CCD camera to capture images. Therefore, in oder to obtain parameters described in section 1.2 one will have to fit a two dimensional gaussian function:

$$f(x,y) = C + A\exp(-\frac{(x-x_0)^2}{2\sigma_x^2} - \frac{(y-y_0)^2}{2\sigma_y^2}) \quad (4)$$

From theoretical model, it is known that the relation between the beam waist and the propagated distance can be obtained either from analysis of

the amplitude (A in Equation (4)) or from the denominator in the exponent's argument. For this analysis, the amplitude will not be used, as its relationship with the beam waist is given by the following equation:

$$w(z) = \sqrt{\frac{2P}{\pi A}} \approx k \cdot \sqrt{\frac{1}{A}},$$

where k is a constant that cannot be determined given the experimental knowledge possessed. Therefore, the chosen approach focused on analyzing the variances σ_x, σ_y from Equation (4) and their relationship with the denominator in Equation (1):

$$-2\frac{r^2}{w(z)^2} = (-\frac{(x-x_0)^2}{2\sigma_x^2} - \frac{(y-y_0)^2}{2\sigma_y^2}).$$

A key assumption was to treat σ_x and σ_y equally and replace them with their mean value:

$$\frac{r^2}{w(z)^2} = (\frac{(x-x_0)^2 + (y-y_0)^2}{4\bar{\sigma}^2}).$$

This approach assumes a circular beam shape, meaning that the analysis excludes astigmatism and focuses on the ideal Gaussian beam model. Consequently, the beam waist function can be approximated as:

$$w(z) = |\sigma_x + \sigma_y|, \tag{5}$$

with the propagated uncertainty u_{wz} being a function of uncertainties in the previously mentioned variances ($u_{\sigma_x}, u_{\sigma_y}$):

$$u_{wz} = \sqrt{u_{\sigma_x}^2 + u_{\sigma_y}^2}. \tag{6}$$

It is worth noting that Equation (1) was not used directly due to the limited number of fitting parameters, which led to insufficient accuracy and long processing times. M-squared parameter was obtained by fitting Equation (2) directly to the results of the previous analysis, using the relation defined in Equation (5).

2 Experiment

The experiment consisted of five main segments, utilizing three different experimental configurations discussed below.

2.1 Beam measurement

The measurement of the beam properties, aimed at determining the M^2 parameter and the beam's waist was conducted using the configuration shown in the Figure 1. The measurement involved

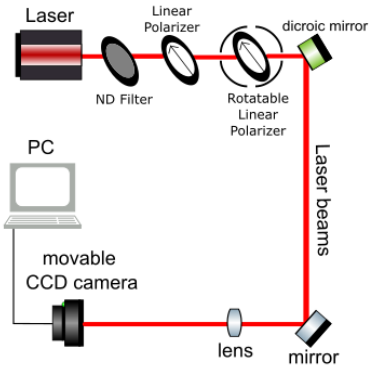

Figure 1: The experimental configuration included Helium–Neon laser, filters, polarizers, mirrors, a converging lens and a CCD camera connected to a PC.

modulating the distance between the camera and the lens to locate the focal point. The objective was to measure points before and after focal point, with the points being denser distributed near focal point. During the measurement, the camera reached saturation on multiple occasions. To prevent data loss, polarizers were used to modulate the beam intensity. When the polarizers were not sufficient enough (near the focal point), the camera's saturation time variable was adjusted. Analogically, after passing the focal point, both the polarizers and saturation time were adjusted to accurately register the intensity.

2.2 Addition of the laser crystal

The beam properties were measured again, this time with the inclusion of a laser crystal, as

shown in Figure 2. The crystal had to be carefully placed in order to avoid distorting the beam. The methodology used was identical to that described in section 2.1.

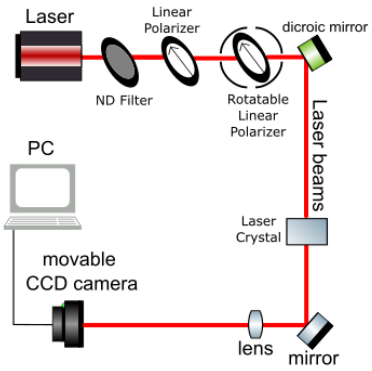

Figure 2: The experimental configuration included Helium–Neon laser, filters, polarizers, mirrors, a converging lens and a CCD camera connected to a PC with addition of a laser crystal.

2.3 Change of lens

After successfully measuring laser beam passing through the laser crystal, the experiment configuration was modified by replacing optical lens with one of a different focal length. The laser crystal was removed, and the measurement was conducted using the configuration shown in Figure 1. The methodology remained identical to that described in section 2.1.

2.4 Change of laser

After taking measurements with the different lens, the Laser source was replaced, with no changes made to the configuration or other optical components. Therefore the configuration in this measurement was the same as that illustrated in Figure 1. The methodology remained identical to that described in section 2.1.

2.5 Measuring astigmatism

In order to measure astigmatism, the configuration was set in a 'Z' pattern, as shown in Figure 3. Despite the different shape, the methodology remained identical to that described in section 2.1, with the only differences being the presence of two focal points instead of one.

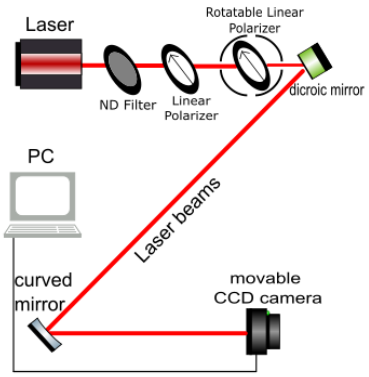

Figure 3: The experimental configuration ('Z') included Helium–Neon laser, filters, polarizers, mirrors, a curved mirror and a CCD camera connected to a PC.

3 Results

3.1 Initial beam measurement

After the careful measurements described in detail in section 2, data analysis was conducted. The CCD camera recorded data in 8 bit BMP files, which had to be decoded and properly plotted to allow parameter extraction via fitting. The plotting and fitting were successful, and the example results are presented in Figures 4, 5.

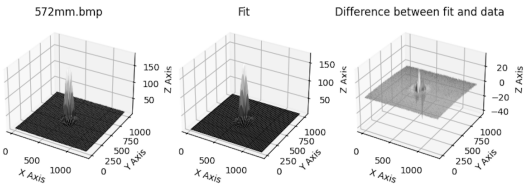

Figure 4: Presentation of the fitting result for data points in the initial beam measurement. The plotted function corresponds to the one shown in equation (4).

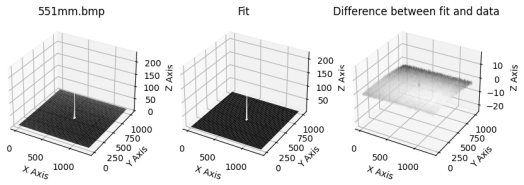

Figure 5: Presentation of the fitting result for data points in the initial beam measurement near the focal point. The plotted function corresponds to the one shown in equation (4).

Similar results were obtained for all points, regardless of the distance from the focal point. Since the analysis of Gaussian beam parameters requires careful examination of the focal point region, this consistency was crucial for later analysis. To proceed with the examination of the beam parameters, the obtained variances were converted to millimeters, assuming that 1 pixel corresponds to 5 µm, and then used to calculate the waist function and its uncertainty using Equations (5), (6). Figure 6 presents the results of the waist function analysis, as described by Equation (2). The z_R parameter was calculated using Equation (3) for $\lambda = 633$ nm.

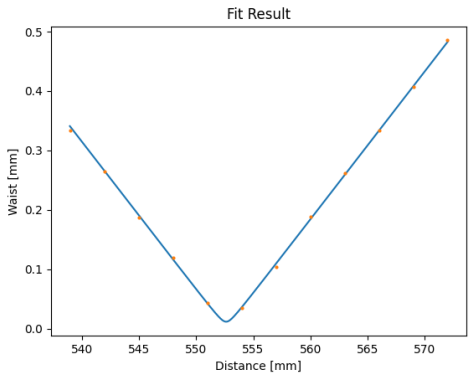

Figure 6: Presentation of the fitting result from the analysis of all valid Gaussian fit parameters for the initial beam measurement. The fitting function used is shown in Equation (2).

The fit results from Figure 6 accurately match the obtained data and can be used to estimate the beam parameters. The fitted parameters are listed in Table 1. The obtained parameters are all within the expected range; however, the high M^2 uncertainty suggest insufficient dataset. The measurement error of the CCD camera and the optical system is difficult to estimate. To improve future measurements, a greater number of points is required. The CCD Camera has a limited spatial resolution and cannot be used for precise measurements if the beam diameter corresponds only to a few pixels, as it is the case near the focal point (Figure 5). According to R. Paschotta's article on 'Gaussian Beams' in the RP Photonics Encyclopedia [2] approximately half of the measurement points must be more than two effective Rayleigh lengths away from the beam focus, while the other half should be close to the focus (within one Rayleigh length). This standard was not adhered to during the measurements, possibly contributing to the instability of the fit. Another possible issue is the frequent adjustment of saturation time and light polarization, which leads to a loss of information about the beam intensity. After modifying these parameters, the points are no longer measured consistently. As a result, the following measurements exhibit similar inaccuracies.

Table 1: Results of data analysis performed on the initial beam sample. The fitted function is represented by Equation (2). The Root Mean Squared Error ($RMSE$) is 0.0033 and the R-squared value is 0.9994.

z_0 [mm]	w_0 [mm]	M^2 [-]
552.627 ± 0.047	0.0115 ± 0.0086	2.0 ± 3.0

3.2 Measurement with laser crystal

Figure 7 presents the results of the waist function analysis based on Equation (2). As discussed in section 3.1, the results accurately represent the physics of the measured phenomenon. The extracted parameters are presented in Table 2.

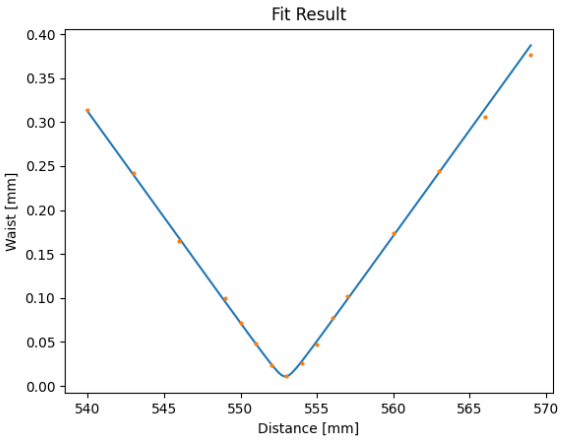

Figure 7: Presentation of the fitting results from the analysis of all valid Gaussian fit parameters for the measurement with a laser crystal. The fitting function used is shown in Equation (2).

Table 2: Results of data analysis performed on the measurement with a laser crystal sample. The fitted function is represented by Equation (2). The Root Mean Squared Error ($RMSE$) is 0.0043 and the R-squared value is 0.9986.

z_0 [mm]	w_0 [mm]	M^2 [-]
552.937 ± 0.036	0.0178 ± 0.0017	1.66 ± 0.53

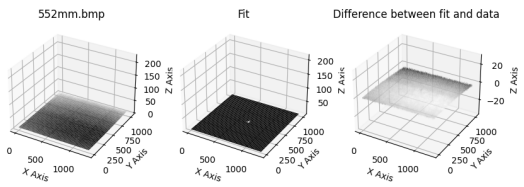

Figure 8: Presentation of the fitting result for data points in the measurement with laser crystal near the focal point. The plotted function corresponds to the one shown in equation (4).

The parameters in Table 2 are within the expected range despite difficulties in fitting the Gaussian beam near the focal point, as presented in Figure 8. However, the M^2 value has significantly lower uncertainty than the initial beam. This is likely caused by an increased number of measurement points, approximately 30 percent more. Notably, there is consistency between the beam waist and the position of its narrowest point in both the initial measurement and this one, which includes a laser crystal, indicating that the beam did not seem to be influenced by passing through the laser crystal. However, the increased M^2 could suggest that the beam quality has improved.

3.3 Measurement after lens alteration

Figure 9 presents the results of the waist function analysis based on Equation (2). As discussed in section 3.1, the results accurately represent the physics of the measured phenomenon. The extracted parameters are presented in Table 3.

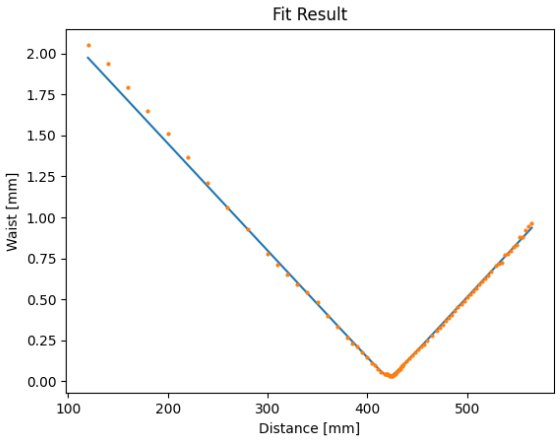

Figure 9: Presentation of the fitting results from the analysis of all valid Gaussian fit parameters for the measurement with a changed lens. The fitting function used is shown in Equation (2).

The parameters in Table 3 are within the expected range. It can be observed that the position and value of the beam's narrowest waist changed when the lens was altered, unlike when the crystal was added. Assuming the lenses had different optical

Table 3: Results of data analysis performed on the measurement with a changed lens sample. The fitted function is represented by Equation (2). The Root Mean Squared Error ($RMSE$) is 0.021 and the R-squared value is 0.9979.

z_0 [mm]	w_0 [mm]	M^2 [-]
421.87 ± 0.16	0.0308 ± 0.0023	1.00 ± 0.15

powers, this outcome is expected. In this measurement, the number of points has been increased by approximately 600% compared to the previous ones, which could lead to the lowest possible value of M^2, which is 1. Other possible causes of improved beam quality could include better calibration of the optical system and the higher quality of the altered lens.

3.4 Beam parameters of another light source

Figure 10 presents the results of the waist function analysis based on Equation (2). As discussed in section 3.1, the results accurately represent the physics of the measured phenomenon. The extracted parameters are presented in Table 4.

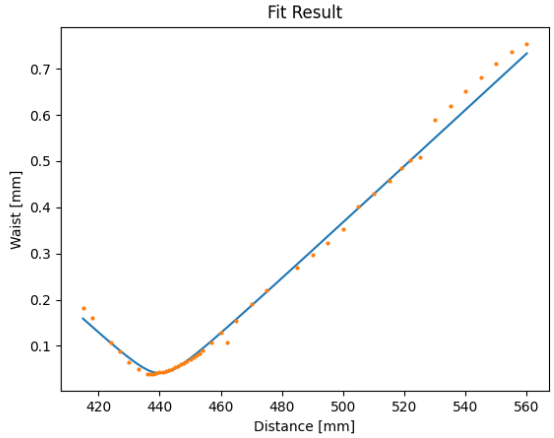

Figure 10: Presentation of the fitting results from the analysis of all valid Gaussian fit parameters for the measurement with a changed light source. The fitting function used is shown in Equation (2).

Table 4: Results of data analysis performed on the measurement with a changed lens sample. The fitted function is represented by Equation (2). The Root Mean Squared Error ($RMSE$) is 0.16 and the R-squared value is 0.9950.

z_0 [mm]	w_0 [mm]	M^2 [-]
440.13 ± 0.28	0.0411 ± 0.0013	1.55 ± 0.11

The parameters in Table 4 are within the expected range. The measurement was conducted with the same optical system as the one used for analysis in section 3.3, but with a different light source, which was expected to have lower beam quality. Consequently, the observed result, a wider narrowest point and higher M^2 value after altering the light source, was anticipated. The shift in z_0 position is likely related to a change in narrowest waist value, assuming the wavelength of the alternative light source was the same.

3.5 Astigmatism analysis

After adding artificial astigmatism to the Gaussian beam by introducing a curved mirror (Figure 3), the fitting function in Equation (2) required proper adjustments for the analysis of the beam with two focal points. To analyze these two focal points separately, it was assumed that the solution is a superposition of two focal points:

$$w(z) = w_{x0}\sqrt{1 + M^2(\tfrac{z-z_{x0}}{z_{xR}})^2} + w_{y0}\sqrt{1 + M^2(\tfrac{z-z_{y0}}{z_{yR}})^2}.$$

Figure 11 presents the results of the waist function analysis based on the superposition from Equation (2). As discussed in section 3.1, the results accurately represent the physics of the measured phenomenon. The extracted parameters are presented in Table 5. It is also considered relevant to note that the background visibly shifts during the measurement with artificial astigmatism, as observed in Figures 12 and 13. This result clearly indicates that the beam was not perpendicular to the CCD camera plane, negatively affecting the measurement. Regarding the fitting parameters extracted and presented in Table 5, the focal

position and waist are once again within the expected range. The beam quality factor has a very low value; however there is a significant increase in uncertainty compared to the previous measurement, likely caused by limited dataset.

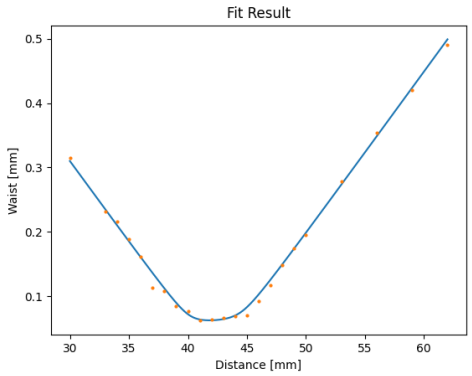

Figure 11: Presentation of the fitting results from the analysis of all valid Gaussian fit parameters for the measurement with artificial astigmatism. The fitting function used is the superposition of the function shown in Equation (2).

Table 5: Results of data analysis performed on the measurement with a artificial astigmatism sample. The fitted function is represented by a superposition of a function in Equation (2). The Root Mean Squared Error ($RMSE$) is 0.0073 and the R-squared value is 0.9963.

z_{x0} [mm]	w_{x0} [mm]	M^2 [-]
40.17 ± 0.42	0.0154 ± 0.0054	1.00 ± 0.67
z_{y0} [mm]	w_{y0} [mm]	M^2 [-]
44.46 ± 0.44	0.0167 ± 0.0061	1.00 ± 0.67

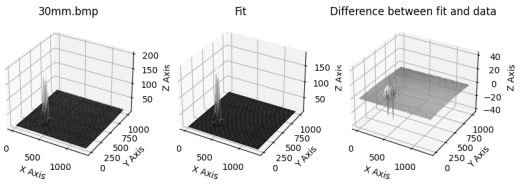

Figure 12: Presentation of the fitting result for data points in the measurement with artificial astigmatism at the beginning of the measurement. The plotted function corresponds to the superposition of the function shown in equation (4).

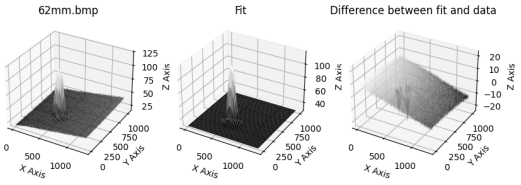

Figure 13: Presentation of the fitting result for data points in the measurement with artificial astigmatism at the end of the measurement. The plotted function corresponds to the superposition of the function shown in equation (4).

References

[1] R. Paschotta, article on "Gaussian Beams" in the RP Photonics Encyclopedia [access: 13.02.2025]

[2] R. Paschotta, article on "M^2 Factor" in the RP Photonics Encyclopedia [access: 13.02.2025]